Comprehensive Control of Resistive Wall Modes in DIII-D Advanced Tokamak Plasmas

M. Okabayashi 1), I.N. Bogatu 2), T. Bolzonella 3) M.S. Chance 1), M.S. Chu 4), A.M. Garofalo 4), R. Hatcher 1), Y. In 2), G.L. Jackson 4), J.S. Kim 2), R.J. La Haye 4), M.J. Lanctot 5), Y.Q. Liu 6), T.C. Luce 4), L. Marrelli 3), P. Martin 3), G.A. Navratil 5), H. Reimerdes 5), E.J. Strait 4), H. Takahashi 1), and A.S. Welander 4)

1) Princeton Plasma Physics Laboratory, Princeton, New Jersey, USA
2) FAR-TECH, Inc., San Diego, California, USA
3) Consorzio RFX, Italy
4) General Atomics, San Diego, California, USA
5) Columbia University, New York, New York, USA
6) UKAEA, Culham, UK

e-mail contact of main author: mokabaya@pppl.gov

Abstract. The resistive wall mode (RWM) and neoclassical tearing mode (NTM) have been simultaneously suppressed in the DIII-D for durations over 2 seconds at beta values 20% above the no-wall limit with modest electron cyclotron current drive (ECCD) and low plasma rotation. The critical plasma rotation was significantly lower than reported at the IAEA FEC in 2006. However, even in this stabilized regime, stable steady-state operation is not unconditionally guaranteed. Various localized MHD activities such as edge localized modes (ELMs) and fishbones begin to couple to the RWM branch near the no-wall limit. Feedback is useful to improve the stability. Simultaneous operation of slow dynamic error field correction and fast feedback suppressed the ELM-induced RWM at high normalized beta. The result implies that successful feedback operation requires careful control of residual RWMs. The effectiveness of feedback operation was demonstrated using a reproducible current-driven RWM. The present findings are extremely useful in the challenge of control of RWM and NTM in the unexplored physics territory of burning plasmas in ITER.

1. Introduction

Comprehensive control of the resistive wall mode (RWM) is a prerequisite for achieving steady-state commercial fusion reactors based on the Advanced Tokamak concept [1]. The RWM is an ideal-kink mode branch, excited due to the finite resistivity of the external wall surrounding the plasma when the plasma pressure expressed by β exceeds the ideal MHD no-wall stability limit, $\beta_{no-wall}$, where β is defined as plasma pressure divided by the confining magnetic pressure. The existence of high beta regimes stable to the RWM and above the no-wall beta limit was successfully demonstrated at low plasma rotation in DIII-D and JT-60U [2–4]. Another global mode, the 2/1 neoclassical tearing mode (NTM), becomes a performance limiting instability at high β_N [$\equiv \beta/(I_p/aB_T)$] by lowering confinement and leading to β_N collapse. Recently, the NTM threshold in DIII-D was found to depend on plasma rotation near the no-wall limit [5]. Numerical simulation has predicted that the NTM can be excited just above no-wall limit without any seed island [6]. When the plasma rotation is as low as expected in ITER, it is possible that these dependences of the RWM and NTM onset on the plasma rotation add to the complexity for identifying and controlling the RWM.

In RWM stability experiments on DIII-D, electron cyclotron current drive (ECCD) has been applied on the q=2 surface to suppress the NTM. Both the RWM and NTM have been simultaneously suppressed for over 2 seconds. The critical rotation for RWM stability was significantly lower than reported in [2,3]. However, even in this stabilized regime, stable steady-state operation is not unconditionally guaranteed. In advanced tokamak plasmas with high q operation, the q=2 fishbone instability excites RWM at low rotation (Fishbone-driven RWM). Even with high plasma rotation, ELM-induced RWM has caused β_N collapse (ELM-driven RWM).

Feedback is useful to improve the stability. In the DIII-D facility, two coil systems are available for separate feedback functions, one with internal I-coils for fast time response

($\tau_{FB} \lesssim \tau_w$) and the other with external C-coils for slow time response ($\tau_{FB} \gtrsim \tau_w$), where τ_{FB} is the feedback time constant and τ_w is the resistive wall time. Simultaneous operation of fast feedback and slow dynamic error field correction is a promising approach [7]. A hypothesis is proposed that the finite amplitude of a residual RWM increases the complexity of the feedback process. A possible process of forming residual RWM is the resonant field amplification of unknown error fields.

The result implies that successful feedback operations require careful control of residual RWM. The complexity of feedback operation at high β_N could also be caused by more fundamental issues such as mode non-rigidity under the presence of non-axisymmetric field, which was studied using the NMA code [8]. The reproducible current-driven RWM (at very low β_N) was utilized to reveal details of feedback process.

2. RWM Stability in the NTM Suppressed Plasmas by ECCD

Pre-emptive NTM suppression by ECCD [9] was applied to high β_N plasmas 20% above no-wall limit, $\beta_{N.no\text{-}wall}$ (~2.5l_i), which targets were used previously for low rotation high β_N plasma exploration [10]. The ECCD power of 2 MW, moderate compared to the 10–13 MW NBI injected power, was sufficient to successfully suppress the NTM. Figure 1 shows a typical discharge with ECCD-NTM suppression where a global mode appeared 500 ms after the ECCD was terminated. The suppression of the NTM made discharges routinely stable at low rotation. A low rotation target was developed by adjusting the combination of co- and counter-NBI power levels to produce plasma rotations as low as possible with a preset-value of β_N. A few discharges were terminated by modes with near zero mode frequency, when the plasma rotation became very low. The RWM grew, coincident with the ELM event, with a growth time of ~10 ms, the same order of magnitude as the wall time, τ_w (ELM-driven RWM). This growth time is consistent with the growth time of RWM theory prediction and similar to the ones previously reported [10].

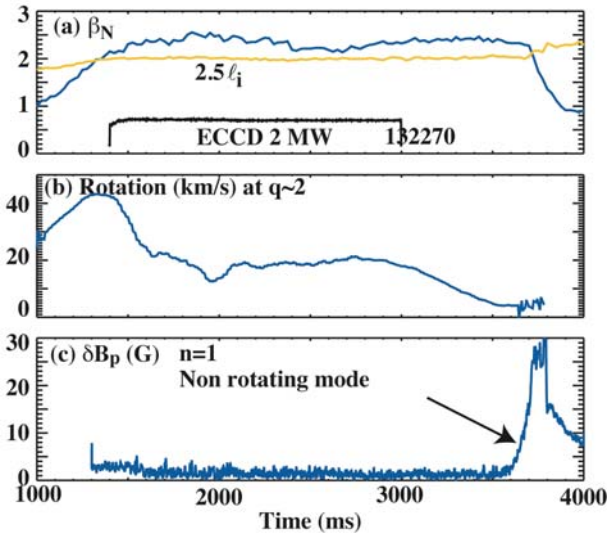

FIG. 1. Long duration RWM/NTM free operation at high β_N by means of ECCD NTM suppression along with RWM control by modest plasma rotation Ω at q~2 (~10–20 km/s, corresponding to $\Omega\tau_A$~ 0.1%–0.2%, where τ_A is Alfvenic time constant). (a) β_N and the estimated no-wall limit $\beta_{N.no\text{-}wall} \cong 2.5\, l_i$, (b) the plasma rotation at q~2, (c) the n=1 δB_p magnitude.

Most of the n=1 MHD activity was excited at lowest rotation several hundred milliseconds after the ECCD was turned off. These modes appeared either with a mode frequency of a few kHz or near-zero. When the mode was rotating, the mode frequency was near the plasma rotation frequency at q=2, implying that the mode is the NTM. An interesting question arises as to whether or not the non-rotating mode belongs to the NTM or RWM branch. The poloidal mode structure of the non-rotating mode was compared to that of the rotating mode (after it had locked) using a poloidal array of saddle loops, and they were found to be virtually identical, suggesting that the rotating and non-rotating modes are the same mode.

Additional information is available from the response of this mode to feedback with proportional-only gain. Figure 2(a,b) shows examples of the mode growth excited with/without feedback. For both cases, the ECCD was shut off at 3000 ms. Without feedback [Fig. 2(a)], a rotating mode was excited around t = 3200 ms with a growth time $1/\gamma$ ~ 60 ms

and with feedback [Fig. 2(b)], the onset of non-rotating mode was around t = 3600 ms with the growth time of ~50 ms. Dependence of the growth time on a feedback parameter, toroidal phase shift, between the observed mode and the feedback response, $\delta\phi_{FB}$, is shown in Fig. 2(c). The growth time does not show any preference to the feedback being on or off, the feedback phase shift, or non-rotating/rotating mode. The growth time of the non-rotating case comparable to that of the rotating mode, and considerably longer than that of the low-rotation ELM-driven RWM. These results support a hypothesis that the final collapsing global mode, as shown in Fig.1(c), is not a RWM but more likely a NTM growing in the absence of rotation.

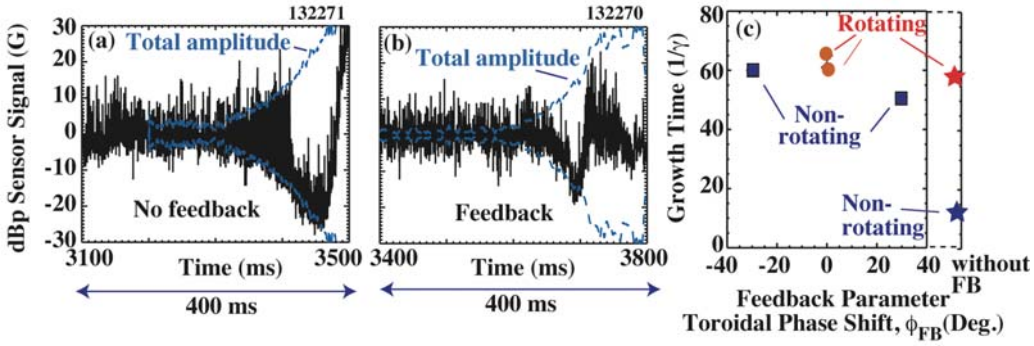

FIG. 2. The mode amplitude along with a δB_p sensor signal (a) without feedback, (b) with feedback. (c) The growth time vs a feedback parameter, toroidal phase shift $\delta\phi_{FB}$. The growth time was averaged over the time period of δB_p from 5 to10 Gauss. The results marked by circles were rotating modes and the ones marked with squares were non-rotating modes. Two shots without feedback (marked with stars) are also included for comparison.

The plasma conditions achieved using NTM suppression with ECCD are summarized in Fig. 3(a) in the dependence of C_β [=$(\beta - \beta_{no\text{-}wall})/(\beta_{ideal\text{-}wall} - \beta_{no\text{-}wall})$] on plasma rotation at q~2. With the appearance of the rotating mode, the critical rotation was similar to the results reported at the IAEA FEC in 2006. When the mode was excited as a non-rotating mode, the critical rotation at q=2 was lower and the flatness of the rotation profile at mode onset was significantly different from the one previously reported except very near the edge [Fig. 3(b)]. These results imply the possible existence of RWM suppression mechanisms even when the plasma rotation is totally absent as proposed in [11]. Another possibility is that the edge electric field, which remains similar in these experiments, can be a determining factor of the RWM onset. Since most of the non-rotating modes were excited with feedback applied, it is possible that the feedback had some impact on the final stage toward zero rotation. However, as shown in Fig. 2(c), there was not much definitive dependence of the growth time on the feedback parameters or the presence/absence of feedback.

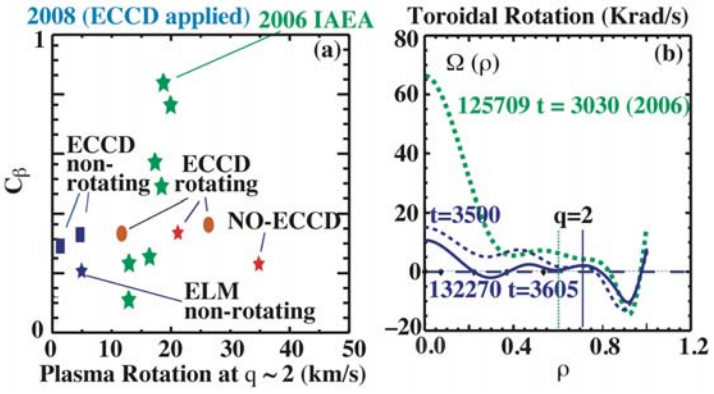

FIG. 3. Achieved C_β vs plasma rotation at q=2 surface. With ECCD NTM suppression, critical rotation at the q=2 surface was near zero. The data were with a rotating mode (circles) and non-rotating mode (squares). Shots without feedback (stars) include several from 2006 for comparison. (b) The rotation profile (#132270) was considerably less-peaked compared with the one (#125709) reported in IAEA 2006.

3. MHD-driven RWM Stability and Feedback

Various MHD events occur in high β_N discharges, producing a wide range of toroidal and poloidal magnetic field patterns. When the RWM stability condition becomes marginal at high beta and low rotation, these fields can interact directly or indirectly with the RWM mode pattern, leading to a rapid, forced excitation of RWM on the time scale of the driving MHD event (MHD-driven RWM). Quite often, the MHD-driven RWM amplitude can be significant, however, the mode itself can remain in marginally-stable regime. On the other hand, this MHD-driven RWM decays very slowly over tens of milliseconds, potentially leading to β_N collapse. Feedback is useful to reduce the mode amplitude before any serious impact takes place.

3.1. *q*=2-Fishbone-induced RWM Stability and Feedback

In the time evolution of the advanced tokamak target, the discharge trajectory passes through regimes vulnerable to various MHD global modes. The *m=2/n=1* *q*=2-fishbone RWM is one of them when q_{min} is ~2. The fishbone at low plasma rotation is quite different from the traditional fishbone of high rotation plasmas. As shown in Fig. 4, when the plasma rotation was kept high enough (e.g., #132270 at $t \sim 1500$ ms) the fishbone bursting period caused little impact on the discharge time evolution (time traces of plasma parameters of #132270 in Fig. 1). When the plasma rotation became lower (at $t \sim 1900$ ms of #131129), the fishbone frequency was reduced, leading to several tens of Gauss RWM onset and β_N collapse at $t \sim 2000$ ms. Before the RWM onset took place, the time-integrated Mirnov signal, δB_p, was strongly distorted [Fig. 4(e)]. The ECE δT_e (ρ~0.5), detected at the same toroidal angle as where the Mirnov loop is located, showed a sharp drop at the time corresponding to the integrated Mirnov signal distortion [Fig. 4(f)]. The source of the distortion observed externally is related to the internal structure located around ρ~0.5, which suggests a "snake-like" magnetic island [12].

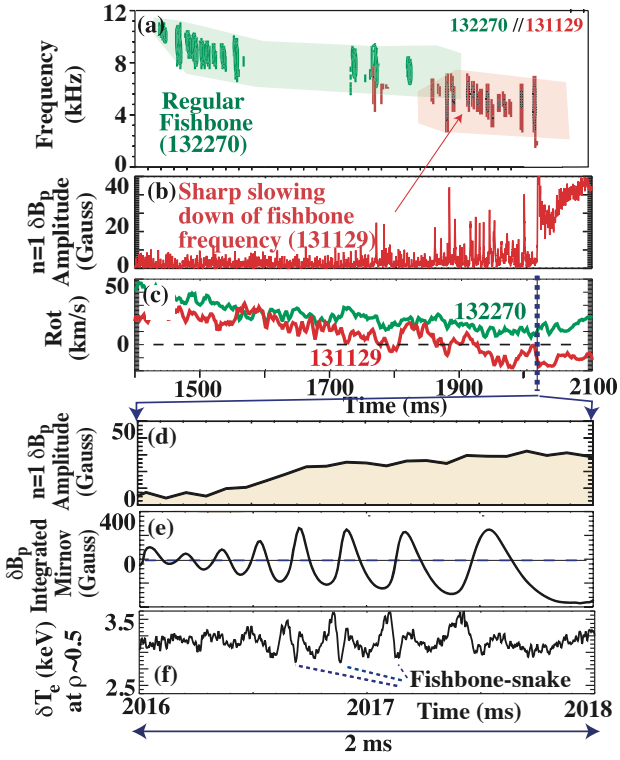

FIG. 4. (a) MHD spectrum of *q*=2 fishbone-like activity with high (#132270) and low (#131129) rotation. (b) the amplitude, (c) the rotation of plasma at *q*~2. The detail of RWM onset (#131129) was shown in (d) the mode amplitude, (e) the Mirnov signal, (f) the ECE signal at ρ~0.5. Sharp distortion of signal δT_e (dotted lines) coincided with the fast change of Mirnov signal.

This snake-like magnetic island is a possibility to enhance the interaction of the (internal kink driven) fishbone and the marginally-stable external kink, exciting the RWM. Another possibility is that the *q*=2 area is covered by both the *q*=2 fishbone and external kink, allowing these mode structures to couple when the rotation of fishbone approaches zero. An interesting result is seen with the application of feedback. Without feedback [Fig. 5(a)], a nearly stationary mode with amplitude ~30 Gauss remains after the last cycle of the *q*=2 fishbone. When the feedback was applied [Fig. 5(b)], a large portion of the mode, dc-like slow *n*=1 component, was suppressed. However, some rotating mode of less than 1 kHz

persisted along with the snake-like distortion seen on the ECE δT_e, indicating that the slow component is a remnant of the internal kink. This slow mode interfered with the feedback process, which gradually requested inordinately-high coil currents.

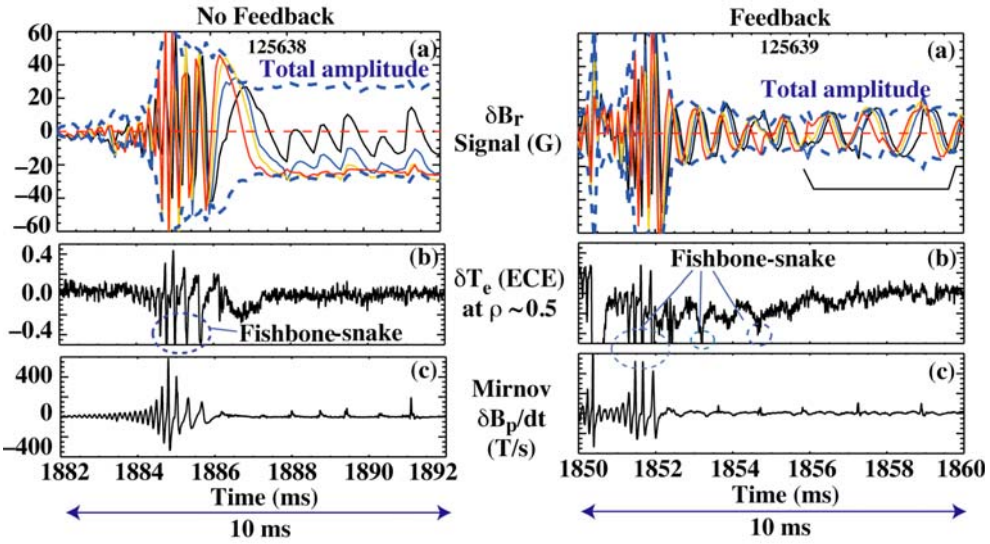

FIG. 5. n=1 fishbone-driven RWM: (left column) without and (right column) with feedback. Application of simple feedback with proportional-gain-only reduced the slow component of q=2 fishbone-driven RWM. (a) δB_p sensor signal, (b) δT_e at ρ~0.5 (toroidal angle = 60°), (c) Mirnov signal (toroidal angle = 67°).

3.2. ELM-induced RWM in High Rotation Plasmas: Stability and Feedback

As reported previously [13], in the high plasma rotation regime the RWMs driven by type-I ELMs are modest with magnitude of 3–10 Gauss and decay times comparable to the resistive wall time scale. Simple feedback operation with proportional-gain-only reduced the RWM amplitude within a fraction of the wall time (~1 ms). The reduction of RWM amplitude led to a reduction of the edge ion temperature disturbances (Fig. 6 shows the case of β_N 20% above the no-wall limit). Without feedback, the ion temperature fluctuated with ΔT_i ~ 0.5–1.0 keV near the edge of the plasma due to 15–20 Hz ELM events, which excited ELM-driven RWMs of 3–5 Gauss. When the feedback was applied, ΔT_i at the top of the H-mode pedestal was reduced to ~0.2 keV as a consequence of the mode amplitude reduction to ~1 Gauss level.

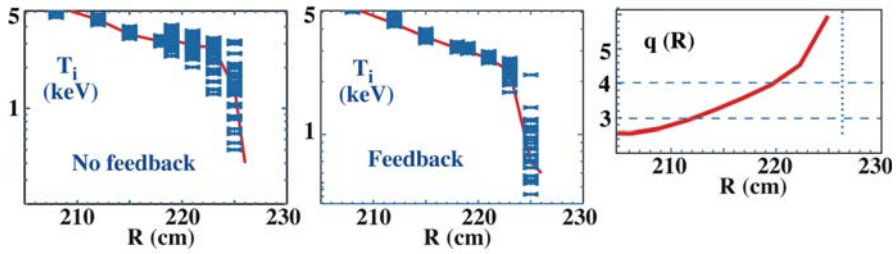

FIG. 6. The edge ion temperature disturbances with/without feedback in a discharge with β_N 20% above the no-wall limit. The statistical variation is shown by overlaying 40 profiles over a time interval of 80 ms.

Too-frequent ELM events can cause difficulty for the feedback. The left column of Fig. 7 shows inefficient feedback when feedback with I-coil-only was applied to a high β_N plasma 20% above the no-wall limit ($\beta_{N.no\text{-}wall}$ estimated ~4l_i). At each ELM event, the feedback, using I-coil currents, tried to reduce the mode amplitude and was successful in holding the

amplitude down to ~2–3 Gauss level with modest current (~ a few hundred Amperes) up to $t \sim 1550$ ms. The requested coil current gradually increased while still sustaining the mode amplitude to a proportionally lower level. However, finally the mode amplitude reached more than 5 Gauss with 1 kA level of coil current, leading to nonlinear stage. A possible process was that this residual RWM grew due to the time-evolving plasma response to a small uncorrected error field. The static error field itself should remain constant on this time scale, ~300 ms, however, the RWM response to the error field could evolve in time. The slow component of I-coil current can be interpreted as the currents needed for suppressing the slowly-time-evolving mode response due to uncorrected error field.

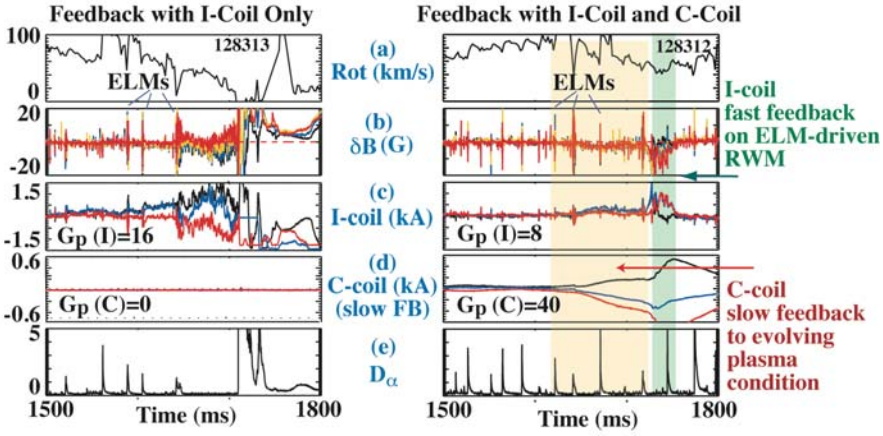

FIG. 7. Frequent ELMs resulted in leading to β_N collapse. (a) Feedback with I-coil-only suppressed the RWM for a few ELMs, however, there was a gradual increase of mode amplitude, which required inefficiently high feedback current. (b) Simultaneous operation with I-coil (fast feedback) and C-coils (slow feedback) reduced the accumulation of RWM amplitude. (a) Plasma rotation at q~2, (b) δB_p sensor signals (c) I-coil currents, (d) C-coil currents, and (e) D_α (au).

A recipe for better control is to separate the feedback process into two functions: one using internal I-coils for fast ELM-driven RWM control and the other using external C-coils for the slow control of the time-evolving plasma response to the growing residual RWM between ELMs. As shown in the right column of Fig. 7, the two coil set arrangement led to better control. The slow increase of feedback coil currents by C-coil replaced the slow rise in I-coil current. When energizing two feedback systems simultaneously, the I-coil dominantly responded to the ELM events with fast time scale. The difference in the two cases is whether the ELM event took place at finite amplitude of slowly-increasing residual RWM or not.

One possible hypothesis is that the formation process of the ELM-driven RWM is affected by the finite amplitude of the residual RWM at the time of ELM events and interferes with the feedback process. Support for this hypothesis was obtained by simulating ELMs with series of n=1 pulses. The use of n=1 pulses is advantageous since the impact is reproducible. The adequacy of simulating ELM with n=1 pulses was confirmed by comparing the decay rates of ELM-driven RWM and the n=1 amplitude excited by n=1 pulses with/without feedback. The response to the applied n=1 pulses was clearly observable [Fig. 8(b,c)], while the amplitude of residual RWM [green shading, Fig. 8(b)] gradually increased. The amplitude and phase of the n=1 plasma response depend on whether the residual RWM exists before the pulse or not as summarized in Fig. 8(d). In particular, the phase shows strong dependence on the residual RWM amplitude. The variation of the n=1 plasma response against the residual RWM is consistent with the hypothesis discussed above.

3.3. Current-driven RWM and Feedback

A challenging issue of exploring RWM stabilization in high β_N plasmas is the non-reproducibility of mode excitation since the high beta RWMs are excited near the operational

maximum β_N. Reproducible current driven-RWM at very low beta was extremely useful to investigate the feedback logic. The mode chosen was the current-driven RWM excited at q_{95}~4 by a strong plasma current ramp, whose helical mode structure is fundamentally same as that with the pressure-driven RWM in AT plasmas.

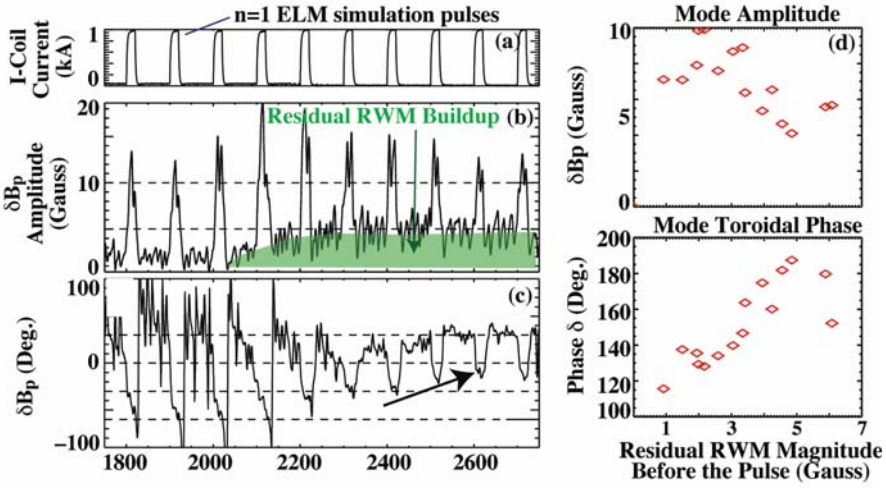

FIG. 8. The n=1 pulses (20 ms pulse width) at every 100 ms were used to simulate ELMs. The δB_p signal shows the gradual increase of residual RWM (green shading) in addition to the response to pulses. (a) The coil currents, (b) δB_p amplitude, (c) toroidal phase angle ϕ, (d) plasma response amplitude and (e) toroidal phase vs the residual RWM level before the pulse applied.

Figure 9 shows the feedback performance, where the mode amplitude at the q_{95}~4 was used as a measure of the mode growth. The increase of proportional gain reduced the mode amplitude to ~2 Gauss level and converted a rotational mode to a non-rotational ω~0 mode. The addition of derivative gain was effective to suppress the mode amplitude. The optimized toroidal phase shift of feedback, $\delta\phi_{FB}$, was non-zero (shifted 20–30 degrees in the plasma current direction). Based on the mode response to the derivative gain and the phase shift, it is believed that the RWM feedback functioned as a direct feedback rather than dynamic error field correction against the static error field.

3.4. Mode Non-rigidity

The feedback functioned as expected in very low β_N current-drive RWM, but in high β_N, the operation was found more difficult as discussed in Sec. 3.2. The complexity of feedback operation at high β_N could be related to more fundamental issues such as mode non-rigidity under the presence of non-axisymmetric field. The mode structure behavior has been studied using the NMA stability code [8], which predicted that feedback can excite a multitude of stable RWMs that couple to the original unstable RWM. This multiple mode involvement can cause a deformation of the mode structure, including the patterns of eddy currents on both the resistive wall and the plasma during the feedback process. The non-rigidity is substantial when the plasma beta is high and the feedback coils are not well matched to the mode structure [Fig. 10(a,b)]. The effect of non-rigidity is minimized by

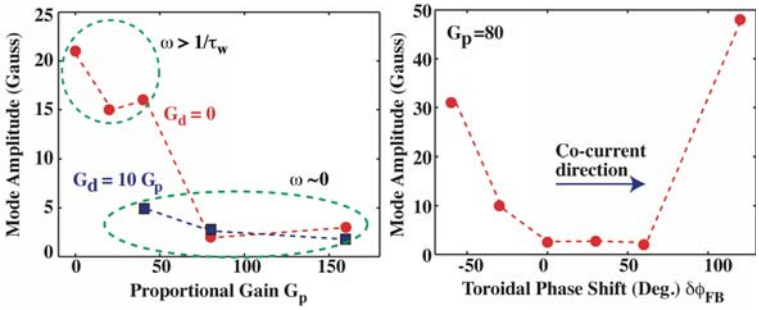

Fig. 9. Feedback performance on the current-driven RWM. (a) mode amplitude at q_{95}=4 vs proportional gain G_p with and without derivative gain G_d, (b) mode amplitude vs toroidal phase shift.

optimizing the coupling of the feedback coils to the primarily unstable RWM, e.g. by using the I-coils [Fig. 10(c)]. The relevance of this phenomenon to ITER is being studied for various proposed alternative feedback coil configurations.

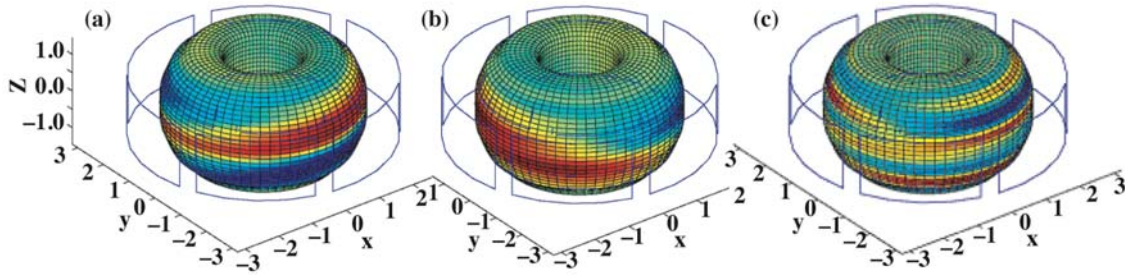

FIG. 10. An example of inefficient feedback configuration with C-coils and improvement with I-coils. Marginal RWM with feedback δB_p pattern on the vacuum wall. Using external C-coil feedback at high β results in large changes to the mode structure. The helicity switches from the left handed helicity of the equilibrium magnetic field to opposite that as β varies from (a) just above the no-wall limit to (b) just below the ideal-wall stability limit. (c) Using I-coil feedback, the mode non-rigidity can be greatly reduced even just below the ideal-wall stability limit.

4. Summary

At very low plasma rotation, the RWM and NTM have been simultaneously suppressed for durations over 2 s with β_N above the no-wall limit, with modest power of ECCD. This result strongly indicates possible existence of RWM stabilization mechanisms in addition to the rotational stabilization. Even when the plasma is stabilized, large amplitude RWMs were transiently excited by MHD activity, such as q=2 fishbones and ELMs. The feedback control was found to be effective in several plasma conditions. Fluctuation of the H-mode pedestal due to ELM-driven RWM was reduced with feedback control. The dominant $\omega\sim0$ component of fishbone-driven RWMs was suppressed, although the rotating component suppression remains a future challenge. Simultaneous fast and slow feedback was successful to reduce the onset of β_N collapse due to the ELM-driven RWM, suggesting that the residual RWM plays a role of hidden parameter. The effectiveness of feedback operation was demonstrated using reproducible current-driven RWM. Using the NMA code, analysis has been carried out to show that better matching of the feedback field pattern to the unstable RWM in high β_N reduces the mode non-rigidity. The present findings are extremely useful to aid in the challenge of comprehensive control of RWM in the unexplored physics territory of the ignited condition in ITER.

This work was supported in part by the US Department of Energy under DE-AC02-76CH03073, DE-FC02-04ER54698, DE-FG02-03ER83657, and DE-FG02-89ER53297.

References

[1] TURNBULL, A.D., *et al.*, Phys. Rev. Lett. **74**, 718 (1995).
[2] GAROFALO, A., *et al.,* Nucl. Fusion **47**, 1121 (2007).
[3] REIMERDES, H., *et al.*, Phys. Rev. Lett. **98**, 055001 (2007).
[4] TAKECHI, M., *et al.*, Phys. Rev. Lett. **98**, 055002 (2007).
[5] BUTTERY, R.J., Phys. Plasmas **15**, 056115 (2008).
[6] BRENNAN, D.P., Phys. Plasmas **9**, 2998 (2002).
[7] GAROFALO, A., *et al.,* Phys. Plasmas **13**, 056110 (2006).
[8] CHU, M.S., *et al.*, Nucl. Fusion **43**, 441 (2003).
[9] PRATER, R., Nucl. Fusion **47**, 371 (2007).
[10] STRAIT, E.J., *et al.,* Phys. Plasmas **11**, 2505 (2004).
[11] HU, Bo., and BETTI, R., Phys. Rev. Lett. **93**, 105002 (2004).
[12] WESSON, J.A., Plasma Phys. Control. Fusion **37**, A337 (1995).
[13] REIMERDES, H., *et al.,* Plasma. Phys. Control. Fusion **49**, B349 (2007).